RSC Advances

ROYAL SOCIETY OF CHEMISTRY

www.rsc.org/advances

Journal Name

ARTICLE

Metal-cladding directly defined active integrated optical waveguide device based on erbium-containing polymer

Received 00th January 20xx,
Accepted 00th January 20xx

DOI: 10.1039/x0xx00000x

www.rsc.org/

Yang Zheng,[a] Changming Chen,*[a] Yunlong Gu,[a] Jihou Wang,[a] Shouzhuo Yang,[a] Xu Fei,[b] Xibin Wang,[a] Yunji Yi,[a] Xiaoqiang Sun,[a] Fei Wang,[a] and Daming Zhang[a]

In this work, metal-cladding directly defined active waveguide technique is proposed. Optical waveguide amplifiers and thermo-optic (TO) waveguide switches based on erbium-containing polymer are designed and fabricated using this technique. The Er organic complexes containing polymeric reactivity groups are synthesized and investigated by free radical copolymerization. Optical characteristics and thermal stabilities of the active polymer are analyzed. Relative optical gain of the amplifier at 1530 nm is obtained as 3.6 dB. The rise and fall response time of the TO switch applied by 300 Hz square-wave voltage are measured as 511.7 μs and 341.5 μs, respectively. The power-time product is 12.5 mW·ms and the extinction ratio is about 20 dB. The technique is very suitable for realizing large-scale optoelectronic integrated circuits.

1. Introduction

Active integrated optical waveguide devices which contain functions of optical amplifiers and thermo-optic switches are key components for reconfigurable optical add-drop multiplexing (ROADM) module in optical cross connect (OXC) networks, which have important applications in optical communication, phase array antennas, optical computer, and optical sensing systems [1-5]. Especially, active polymer waveguides could offer a unique highly integrated optical signal processing platform with benefits of low loss, compact, flexible design of optical properties, and cost-effective features for high-density integrated devices [6-8]. As a multi-functional material system, active polymers exhibit well-controlled refractive indices, highly flexible structures, and large thermo-optic (TO) and electro-optic (EO) coefficients [9-14], which can be advantageous to reduce manufacturing costs and open possibility of monolithic integration with functional devices such as optical amplifiers and switches. Several techniques, such as reactive ion etching [15], light-induced writing [16], laser writing [17], poling-induced writing [18], strain-inducing [19] and molding/embossing [20], have been developed to define optical waveguides in active polymers. In this paper, we demonstrate a novel waveguide defining method that uses a metal-cladding confinement structure to directly produce multi-functional integrated photonic chip based on erbium-containing polymers. Compared with other optical waveguide fabricating methods [15-20], the metal-cladding directly defined waveguide technique could provide a simple, rapid and controllable fabricating process for active integrated photonic device with low-cost, good-performance and effective-yield. Furthermore, compared to other Er-doped polymers [21], as the active core layer, Er complexes are bonded into the copolymer, which is advantageous for the complexes to uniformly disperse into the crosslink polymer avoiding phase separation. Optical absorption characteristics and thermal stability of the cross-linked polymer were obtained. Optical properties of the active waveguide device were analyzed, simulated, and measured. The technique is advantageous to realize a flexible fabrication process for the large-scale photonic multi-functional integrated circuits (PICs) and optimize cross-connectors for OXC and OADM systems.

2. Experimental section

2.1 Waveguide material

2-Thenoyltrifluoroacetone (TTA), 1,10-phenanthroline monohydrate (Phen) and erbium oxide (Er_2O_3) were purchased from J&K, Da Mao Reagent (Tianjin, China), Jin Cheng Yuan Co., and Aldrich (USA) respectively. Methacrylic acid (HMA), Methyl methacrylate (MMA), glycidyl methacrylate (GMA) and other reagents were purchased from SCR (Shanghai, China) and Aladdin. They were used without further purification. 2,2'-Azobisisobutyronitrile (AIBN), recrystallized freshly, was used as a free-radical initiator. Copolymers were obtained by free-radical polymerization of dilute monomer solutions. All of the solvents were used after purification according to conventional methods. A total of 0.01 mol (3.825 g) of Er_2O_3 was dissolved in 40 mL of hydrochloric acid (HCl, 35 wt%) under stirring at 100 °C. The product Er chloride hexahydrate ($ErCl_3 \cdot 6H_2O$) was obtained after evaporating excess HCl, washing with deionized water, and drying under vacuum. Finally, the product was obtained as a pink crystal.

[a] State Key Laboratory on Integrated Optoelectronics, College of Electronic Science and Engineering, Jilin University, 2699 Qianjin Street, Changchun 130012, China. E-mail: chencm@jlu.edu.cn
[b] Instrumental Analysis Center, Dalian Polytechnic University, Dalian 116034, China

As shown in Fig. 1(a), TTA (0.889 g, 4 mmol) and Phen (0.396 g, 2 mmol) were dissolved in ethanol (30 ml, 95%) and then mixed with HMA liquid (0.207 g, 2.4 mmol) in a three necked flask. The obtained solution was stirred and purged under N_2 at 50 °C. The pH value was carefully adjusted to 7.0–7.5 by adding 1 M NaOH in ethanol solution. After 30 min, 30 mL of 66.67 mM $ErCl_3$/ethanol solution was added slowly. With the addition of $ErCl_3$, the precipitate increased. The pH value of the mixed solution must be maintained between 7.0 and 7.5. The obtained solution was purged under N_2 for 20 h. The resulting complex $Er(TTA)_2(Phen)(MA)$ was separated by using centrifugation and rinsed with ethanol several times. The product was dried under vacuum to preserve it.

The molecular structure and synthesis process of the Er-containing copolymer are given in Fig. 1(b). $Er(TTA)_2(Phen)(MA)$ (ErTPM) (0.9 g, 1 mmol), GMA (4.4 g, 31 mmol), MMA (3.1 g, 31 mmol) and AIBN (0.15 g, 0.91 mmol) were dissolved in N,N-dimethylformamide (DMF, 40 mL) with stirring under a nitrogen atmosphere. The resulting solution was then heated at 70 °C for 6 h. The above-mentioned mixture was transferred to a 500 mL beaker containing 200 mL of methanol under stirring. The flocculent precipitate was separated by using centrifugation. The resulting polymer was dissolved in tetrahydrofuran (THF) and purified by precipitation in methanol, this procedure was repeated three times. The product (Er^{3+}, 2 wt%) was then dried under vacuum. The yield of the copolymer was more than 90%. The molecular weight (Mn) was 38000 and polydispersity (PD) was 1.82.

The complex ErTPM is polymerized with MMA and GMA by free-radical polymerization of dilute monomer solutions. The copolymers Poly(GMA-co-$Er(TTA)_2(Phen)(MA)$) (GETPM) could form a highly epoxy cross-linked matrix structure, Which exhibits good chemical resistance and excellent processability. Specific synthesis method and properties of the copolymer are given as ref. [22]. By introducing an organic ligand (methacrylic acid) with excellent polymerization activity, it can provide carboxyl groups as coordinating groups for Er^{3+}. Methacrylic acid plays a dual role as an organic ligand and a compatibilizer and Er chelates can use olefinic double bonds to copolymerize with other monomers for reducing phase separation effectively between Er complexes and polymers. There is low absorption for the Er-containing crosslinking polymer at 1310 nm and 1550 nm wavelength bands based on the near-infrared absorption spectrums of the Er-containing polymer. T_g is the glass transition temperature of Er-containing polymer measured as 142 ℃ by differential scanning calorimetry (DSC); T_d is the onset temperature for 5% weight loss of the polymer measured as 303 ℃ by thermal gravity analysis (TGA), respectively. The morphology and surface uniformity of the cured Er-containing polymer are measured by atomic force microscopy (AFM) and the root-mean-square surface roughness is 0.295 nm. These characteristics of the polymer material are suitable to improve the performances of the integrated optical waveguide device which are contributed for optical communications.

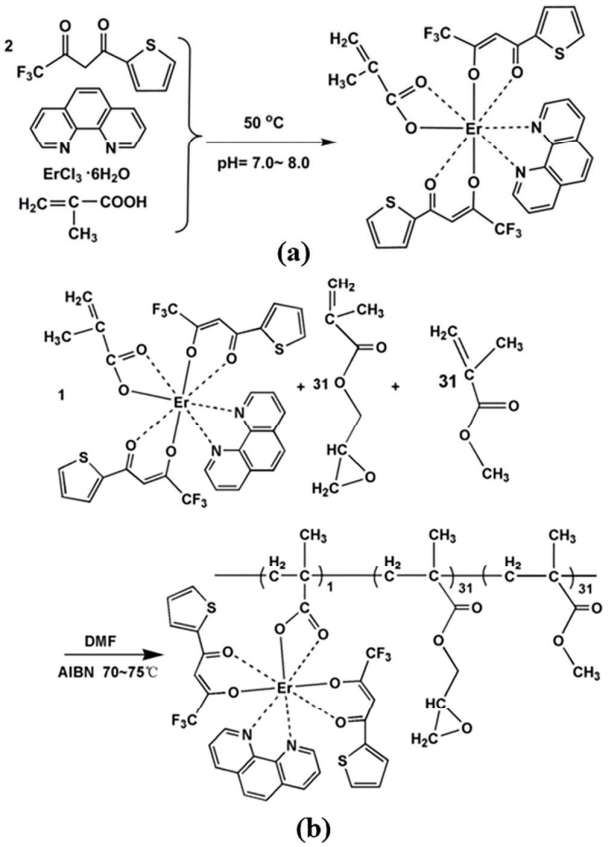

Fig. 1. Synthetic routes to (a) complex ErTPM and (b) copolymer GETPM.

In addition to 2 wt% concentration of Er^{3+} in the cross-linkable copolymer, other samples with different mass fractions of 1 wt% and 2.5 wt% Er-containing polymers were prepared by using a similar method and under the same experimental conditions. The typical emission spectra of 1 wt%, 2 wt% and 2.5 wt% concentration Er-containing polymers were investigated as a KBr pellet (1 wt%) at room temperature, and the characteristic emissions from the Er^{3+} excited state were observed as Fig. 2. The wavelengths of excitation were 390 nm. The emission spectra exhibit characteristic emissions in the region of 430–600 nm after the transitions of $4F_{5/2} \rightarrow 4I_{15/2}$, $4F_{7/2} \rightarrow 4I_{15/2}$, and $4S_{3/2} \rightarrow 4I_{15/2}$ from Er^{3+}. It can be found that 2 wt% concentration Er-containing polymer emits stronger characteristic luminescence than 1 wt% and 2.5 wt% samples in solid states was excited at 390 nm. The reason may be that at low concentrations, luminescence intensity increases with increasing Er^{3+} concentrations. Above the critical point, the luminescence intensity will decrease because of luminescence-quenching occurring within the aggregates of Er^{3+} in GETPMs. We chose GETPM with 2.0 wt% Er^{3+} as the target product with the optimum proportion because of its aggregation and strong luminescence intensity.

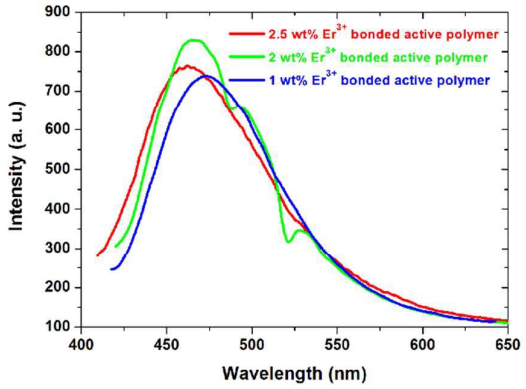

Fig. 2. Emission spectra for 1 wt%, 2 wt%, and 2.5 wt% Er-containing copolymers in solid states was excited at 390 nm.

Figure 3 shows infrared emission spectrum of (Poly(GMA-co-Er(TTA)$_2$(Phen)(MA)) at room temperature with the excitation of a 480 nm laser diode. The 2 wt% concentration of Er^{3+} in the cross-linkable copolymers has a great effect on the emission peak at 1530 nm, which is assigned to the $4I_{13/2}\rightarrow4I_{15/2}$ transition of Er^{3+}. It is conducive to realize fixed infrared signal light power amplification with the role of pump light.

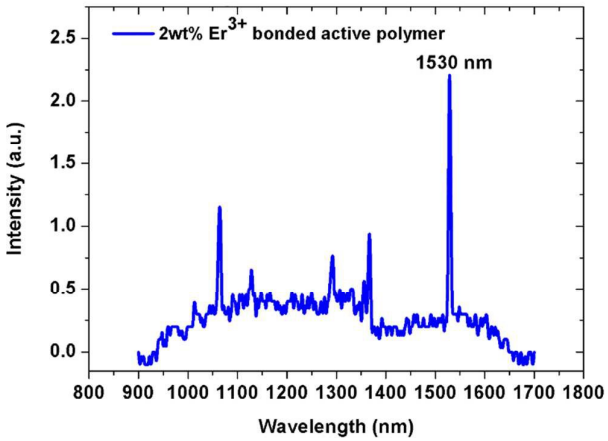

Fig. 3. NIR photoluminescence spectra for Poly(GMA-co-Er(TTA)$_2$(Phen)(MA)) in solid states at a excitation wavelength of 480 nm (75 mW mm^2).

2.2 Waveguide design and fabrication

Figure 4(a) shows the cross-sectional structure of the metal-cladding defined waveguide. Thermally oxidized silicon wafers were used as substrates, with 5 μm thick oxide layer acting as the lower cladding layer. The thickness of Er-containing polymer is 3 μm after spinning-coating onto silicon substrate and heating at 120 ℃. Double parallel Au strips with 0.3 μm thickness and 10 μm width and were formed as metal-upper claddings by deposition, photolithography and wet etching technique. The active optical waveguide structure is directly defined with air-upper cladding layer between the Au strips. The refractive indices of SiO_2, Er-containing polymer, Au and air are 1.450, 1.505, 0.559+11.5i and 1.00 at 1550-nm wavelength, respectively. The mode distribution calculated by software COMSOL multiphysics is shown as Fig. 4(b). The relative eigenvalue equations based on effective index method [23] are defined as

$$k_0(n_1^2-N_1^2)^{1/2}b = n\pi + \arctan\frac{n_1^2(N_1^2-n_2^2)^{1/2}}{n_2^2(n_1^2-N_1^2)^{1/2}} + \arctan\frac{n_1^2(N_1^2-n_3^2)^{1/2}}{n_3^2(n_1^2-N_1^2)^{1/2}}$$

$$(n = 0,1,2,\cdots)$$

$$k_0(n_1^2-N_2^2)^{1/2}(b-h) = n\pi + \arctan\frac{n_1^2(N_2^2-n_2^2)^{1/2}}{n_2^2(n_1^2-N_2^2)^{1/2}} + \arctan\frac{n_1^2(N_2^2-n_3^2)^{1/2}}{n_3^2(n_1^2-N_2^2)^{1/2}}$$

$$(n = 0,1,2,\cdots)$$

$$k_0(N_1^2-N^2)^{1/2}a = m\pi + 2\arctan\frac{(N^2-N_2^2)^{1/2}}{(N_1^2-N^2)^{1/2}}$$

$$(m = 0,1,2,\cdots)$$

where n_1 is the refractive index of the core ridge waveguide, n_2 is the refractive index of the bottom cladding, n_3 is the refractive index of the top cladding, a is the width of the ridge waveguide, h is the height of the ridge waveguide, b is the thickness of the ridge waveguide, N_1 and N_2 are equivalent refractive indices of different regions, respectively.

The equivalent refractive index of both-side waveguides with metal-upper cladding is 1.4791-1.91×10^{-5}i, and that of core waveguide with air-upper cladding is 1.4823. The fundamental mode effective index n_{eff} is 1.4803+6.586729×10^{-6}i. The imaginary part of the effective refractive index is so small that it is ignored in the design of waveguide device.

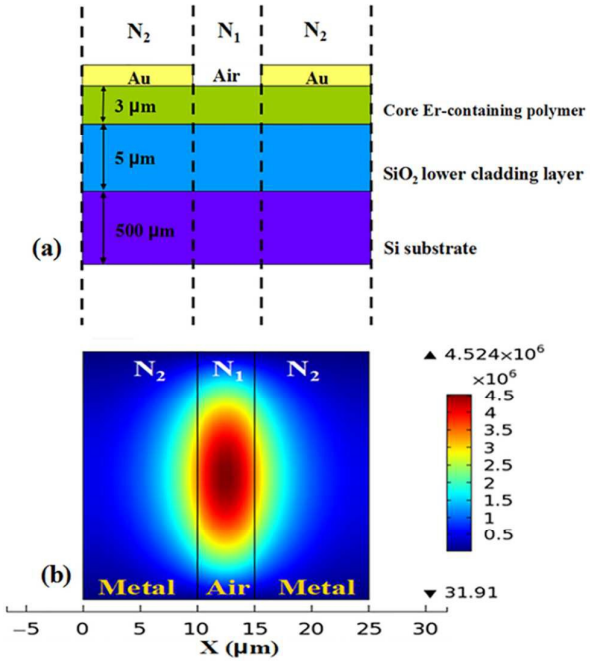

Fig. 4. (a) Cross-sectional structure of the metal-cladding defined waveguide and (b) mode distribution calculated based on effective index method.

The direct optical waveguide amplifier and 1×1 MMI TO waveguide switch are designed and fabricated by the metal-cladding directly defined active waveguide technique. As shown in Fig. 5, the purpose is to realize flexible monolithic multi-functional waveguide chip integrated with amplifying and switching properties.

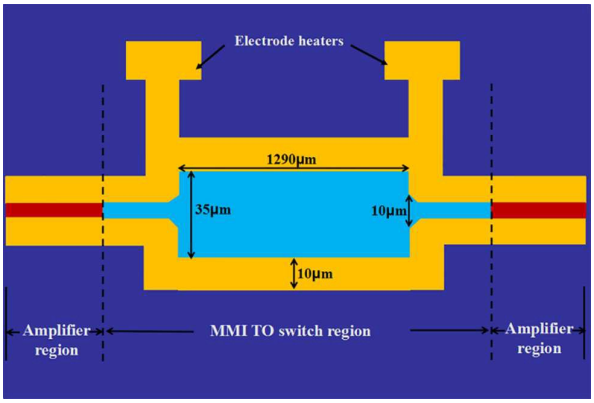

Fig. 5. Schematic configuration of monolithic multi-functional waveguide chip integrated with amplifying and switching properties.

Detailed fabrication process of the metal-cladding directly defined active waveguide device are shown as Fig. 6. The thin film was then cured at 120 ℃ for 1 h to achieve epoxy cross-linked network with 2-methylimidazole as initiator and remove any traces of solvent. The gold film was deposited onto the Er-containing polymer core layer by vacuum evaporation technique. The deposition time was 1 min and the vacuum reached 1.3×10^{-3} Pa. After that, the BP212 photoresist was spin-coated on the gold film and pre-baked at 85 ℃ for 20 min to remove solvent. The gold claddings with self-electrode structure were directly patterned using BP212 photoresist by photolithography and development. The pattern exposure was performed at a 365 nm wavelength and 350 mW Hg lamp power by ABM high resolution mask aligner and exposure system with output intensity as 20 mW/cm^2 and exposure time as 6 s. The BP212 photoresist on the exposure area is removed in 5‰ NaOH solution and the gold claddings with self-electrode structure were formed in I_2 (1 wt%)+KI (4 wt%) developer at room temperature. Finally, The BP212 photoresist on the gold cladding was also exposed and removed in 5‰ NaOH solution. The metal-cladding directly defined waveguide process for the active device based on the Er-copolymer film has the advantage with a small number of steps apt for realizing high reproducibility of the sample fabrication.

Figure 7(a) gives structural patterns of double gold claddings and waveguide region by microscope (×1000). It shows that the parameters designed of the metal-cladding directly defined active waveguide can be realized well and the process enables precise control of the core size. Figure 7(b) gives the surface morphology from the gold cladding measured by AFM. The thickness is about 60 nm and the surface roughness less than 1.5 nm.

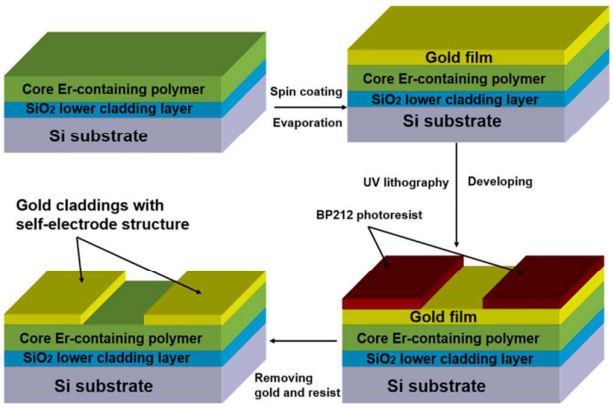

Fig. 6. Fabrication process for metal-cladding directly defined waveguide structure.

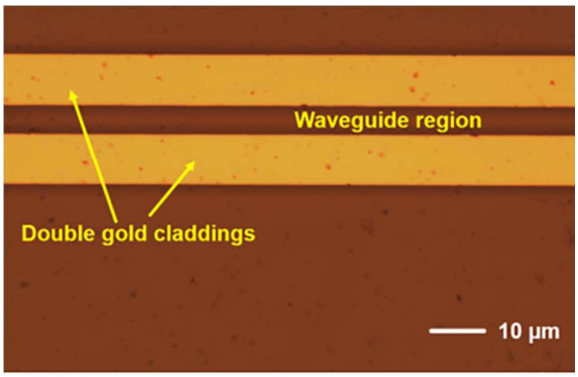

(a)

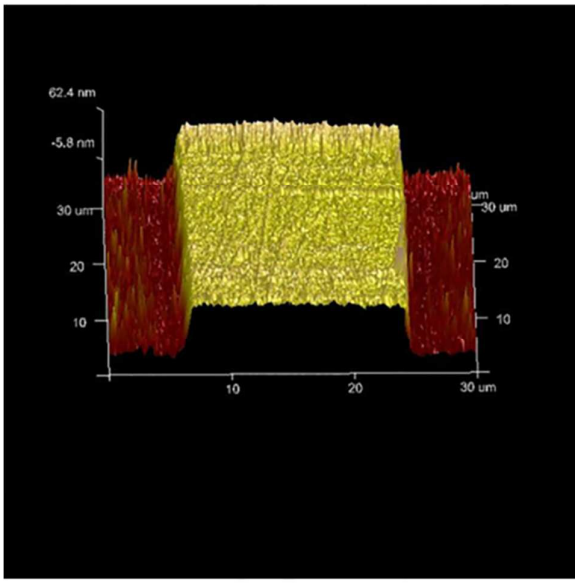

(b)

Fig. 7. (a) Structural patterns of double gold claddings and waveguide region by microscope (×1000) and (b) surface morphology from the gold cladding measured by AFM.

2.3 Device measurement and discussion

For measuring the optical gain of the polymer direct waveguide amplifier, a tunable laser source (Santec TSL-210) with wavelength ranges from 1510 nm to 1590 nm was used as the signal source and a 980 nm laser diode with a maximum output power of 400 mW was used as the pump source. Signal and pump light were launched into the channel waveguides by a 980/1530 nm wavelength division multiplexing (WDM) coupler. The output light from the device was collected and coupled to an optical spectrum analyzer (OSA, ANDO AQ-6315A). The transmission loss of the waveguide with 3 μm width was measured as 2.5 dB/cm by a cut-back method. Figure 8 shows the relative gain with increasing pump power at 1530 nm signal wavelength and the near-field pattern of the device. For an input signal power of 1 mW, the relative gain of the waveguide amplifier increased with the increasing the pump power. When pump power was 100 mW, the maximum relative optical gain at 1530 nm was obtained ~3.6 dB in a 5 mm-long waveguide. The relative gain of the amplifier can realize loss compensation for integrated optical waveguide circuits.

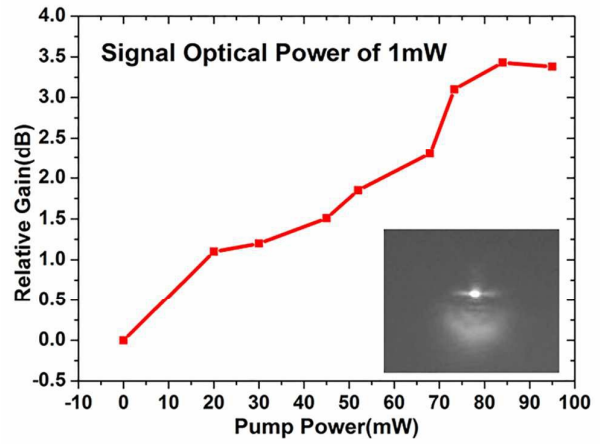

Fig. 8. Relative gain with increasing pump power at 1530 nm signal wavelength and the near-field pattern of the device.

In comparison with key performance parameters of the other reports [24-26] is shown as Table 1. It could be observed that the proposed polymer waveguide amplifier based on Poly(GMA-co-Er(TTA)$_2$(Phen)(MA)) waveguide material could achieve stable operation well with higher relative gain by metal-cladding directly defined technique. Compared with directly doping Er organic complexes, the Er-containing polymer by free radical copolymerization can increase Er^{3+} concentration in polymer matric and prevents degradation of the performances for the optical amplifier.

Table 1 Comparison with other published results for polymer waveguide amplifier

APWMs	WL (mm)	RG (dB)	Reference
LaF_3:Er,Yb–LaF_3/SGHM	17	3.5	[24]
$NaY_{78\%}F_4$: $Yb_{20\%}Er_{2\%}$/KMBR	16	7.7	[25]
β-$NaLuF_4$:Yb^{3+}, Er^{3+} NCs/SU-8	12	2.413	[26]
Poly(GMA-co-Er(TTA)$_2$(Phen)(MA))	5	3.6	Present work

APWMs= active polymer waveguide materials; WL=waveguide length; RG=relative gain

1×1 multimode interference (MMI) TO switch are also realized based on Er-containing copolymers by the metal-cladding defined technique. The structural diagram of 1×1 MMI switch device is constructed, as shown in Fig. 9 (a). Based on the MMI self-imaging theory [27], the length and width of MMI waveguide region is designed as 1290 μm and 35 μm, respectively. A taper structure enables both ends of the MMI waveguide to be connected to the single-mode input and output waveguides so that the switch can transmit optical signals adiabatically without any optical loss. The taper waveguide was optimized and defined as a length of 150 μm and an end width of 10 μm. The width of the gold electrode heater is designed as 10 μm, the width of input and output waveguide is designed as 5 μm and an actual core size of 3×5 μm^2 is obtained for the waveguide device. The TO coefficient of the Er-containing polymer was measured as -1.65×10^{-4} ℃$^{-1}$. The thermal conductivity of the SiO_2 buffer layer and active polymer was 0.27 and 0.16 $Wm^{-1}K^{-1}$, respectively. Figure 9(b) illustrate the optical field transmission Rsoft simulation results of the switch characteristics before and after thermal modulation, respectively. A square-wave voltage was applied to the electrode heater of the actual MMI TO switch with two needle-like probes. The measured total resistance was 300 Ω. The output signal light from the switch was coupled into a photodiode detector and observed using an oscilloscope.

Figure 10(a) shows the TO switching response observed by applying square-wave voltage at a frequency of 300 Hz. The rise and fall times were 511.7 and 341.5 μs, respectively, and the average switch on–off time was about 400 μs. Figure 10(b) shows the channel output intensity versus power consumption of the optical switch at 1550 nm for E_{00}^{x} mode. The extinction ratio of the TO switch was about 20 dB. The applied electric power as the switching power was 23.5 mW, and the corresponding temperature increment of the electrode was 15 K.

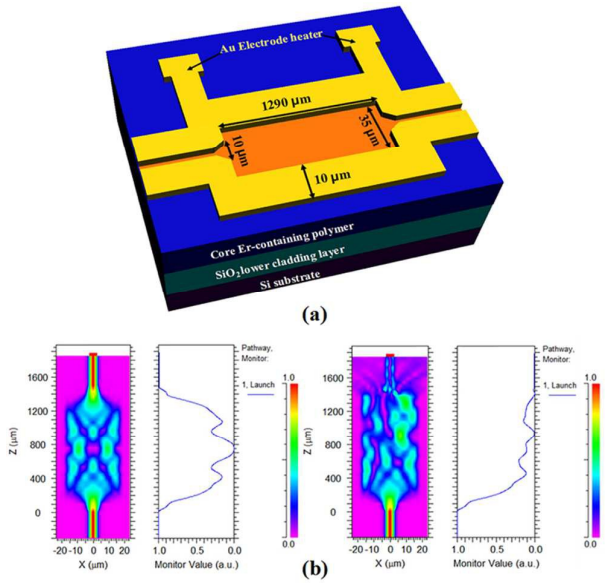

Fig. 9. (a) The structural diagram of 1×1 MMI TO switch device and (b) the optical field simulation of the switching characteristics before and after thermal modulation, respectively.

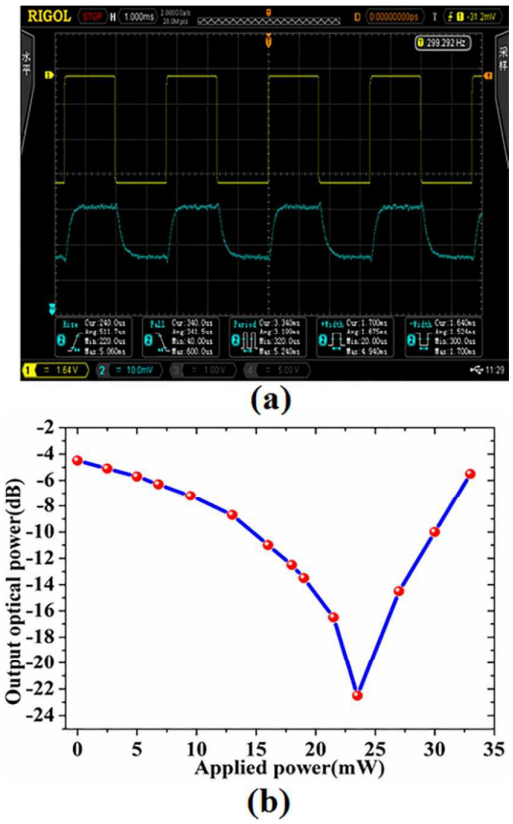

Fig. 10. (a) Switch responses and (b) actual channel output versus power consumption of the MMI TO switch.

Compared with the reported polymer 1 × 1 MMI TO waveguide device [28–31], including our work, the extinction ratio was obtained mainly in the range of 20~30 dB. The other parameter values of the device length and the switching power-time product were put into perspective by comparison with the performance of the polymer MMI TO device published in the literature, given in Table 2. It can be observed that the proposed 1 × 1 MMI TO device could achieve stable operation well with a smaller size and a lower power-time product. The advantages of the performances from the overall device can be obviously noted. In addition, the metal-cladding directly defined active waveguide technique without an etched or diffused process is more convenient for realizing integrated photonic circuits.

Table 2 comparison with other published results for polymer 1×1 TO MMI device

In×Out	Lengh (mm)	Power-Time product (mW·ms)	Reference
1×1	10	203	[28]
1×1	6	31.2	[29]
1×1	15	550	[30]
1×1	0.65	202	[31]
1×1	3	12.5	Present work

For the stability of the active devices, there is no any damage phenomenon found in the amplifier with the maximum 980 nm pump power of 400 mW. Two months later, the response characteristics of the MMI TO switch were re-tested. Under the same testing condition, there was no attenuation of amplitude and hysteresis of switch time. For the durability of the active devices, the steady operating states of the amplifier and MMI TO switch were maintained and continuously enhanced the working temperature in the range of 25–85 °C held for 20 hours. There was no significant effect on performances of the active devices during the various reliability tests. The reasons for these findings may be that 3D network of Er crosslinking copolymer forms a protective barrier against thermal decomposition while ensuring good stability and durability.

3. Conclusions

In summary, we have demonstrated that new types of optical waveguide amplifiers and MMI TO waveguide switches based on erbium-containing polymer are achieved using novel metal-cladding directly defined technique. The technique could provide a simple, rapid and controllable fabricating process for multi-functional integrated photonic chips and be potential for surface plasmon polariton (SPP) waveguide applications. The core copolymers GETPM could form a highly epoxy cross-linked matrix structure, which exhibits good chemical resistance and excellent processability. By introducing an organic ligand (methacrylic acid) with excellent polymerization activity, it can provide carboxyl groups as coordinating groups for Er^{3+}. Methacrylic acid plays a dual role as an organic ligand and a compatibilizer and Er chelates can use olefinic double bonds to copolymerize with other monomers for reducing phase separation effectively between Er complexes and polymers. The optical properties of the active polymer were analysed. T_g and T_d of the Er copolymer are measured as 142°C and 303 °C, respectively. The GETPM

with 2.0 wt% Er^{3+} are chosen as the target product with the optimum proportion because of its aggregation and strong luminescence intensity. Relative optical gain of the amplifier at 1530 nm was obtained as 3.6 dB in a 5 mm-long waveguide. The characteristic parameters of the MMI TO switch were carefully designed and simulated. The Power-Time product was 12.5 mW·ms and the extinction ratio was about 20 dB. This technique is advantageous to improve cross-connectors for the optoelectronic integrated circuits.

Acknowledgements

The authors gratefully acknowledge financial support from National Natural Science Foundation of China (No. 61107019, 61475061, 61405070, 61177027, 61275033, 61205032, 61261130586), Ph.D. Programs Foundation of Ministry of Education of China (No. 20110061120054, 20130061120060), Science and Technology Development Plan of Jilin Province (No. 20130522151JH,20140519006JH),The Fundamental Research F unds for the Central Universities (No. JCKY-QKJC08) and National Undergraduate Training Programs for Innovation and Entrepreneurship (No. 2015510624).

References

1 Toru Segawa, Shinji Matsuo, Takaaki Kakitsuka, Yasuo Shibata, Tomonari Sato, Yoshihiro Kawaguchi, Yasuhiro Kondo and Ryo Takahashi, Opt. Exp., 2010, **18**(5), 4341–4345.
2 Francesca Bontempi, Sergio Pinna, Nicola Andriolli, Antonella Bogoni, Xaveer J. M. Leijtens, Jeroen Bolk, and Giampiero Contestabile, IEEE J. Quantum Electron, 2012, **48**(11), 1453–1461.
3 Wanjun Wang, Haifeng Zhou, Jianyi Yang, Minghua Wang and Xiaoqing Jiang, Optics Lett., 2012, **37**(12), 2307-2309.
4 Francesca Bontempi, Stefano Faralli, Nicola Andriolli, and Giampiero Contestabile, Photon. Technol. Lett., 2013, **25**(22), 2178–2181.
5 Mulham Khoder, Guy Verschaffelt, Romain Modeste Nguimdo, Xaveer Leijtens, Jeroen Bolk and Jan Danckaert, Optics Lett., 2013, **38**(14), 2608-2610.
6 Changming Chen, Xiaoyan Niu, Chao Han, Zuosen Shi, Xinbin Wang, Xiaoqiang Sun, Fei Wang, Zhanchen Cui, and Daming Zhang," Opt. Exp., 2014, **22**(9), 10716-10727.
7 Young-Tak Han, Jang-Uk Shin, Sang-Ho Park, Jun-Kyu Seo, Hyung-Jong Lee, Wol-Yon Hwang, Hyo-Hoon Park, and Yongsoon Baek, IEEE Photon. Technol. Lett., 2012, **24**(19), 1757–1760.
8 Changming Chen, Feng Zhang, Hui Wang, Xiaoqiang Sun, Fei Wang, Zhanchen Cui and Daming Zhang, IEEE J. Quantum Electron., 2011, **47**(7), 959-964.
9 Nikolaos Bamiedakis, Joseph Beals, IV, Richard V. Penty, Ian H. White, Jon V. DeGroot, Jr., and Terry V. Clapp, IEEE J. Quantum Electron, 2009, **45(**4), 415–424.
10 Jialei Liu, Guangming Xu, Fenggang Liu, Iwan Kityk, Xinhou Liua and Zhen Zhen, *RSC Adv.*, 2015,**5**, 15784-15794.
11 Wenbin Huang, Linsen Chen and Li Xuan , RSC Adv., 2014,**4**, 38606-38613.
12 Jingdong Luo, Xing-Hua Zhou and Alex K.Y. Jen, Journal of Materials Chemistry, (2009), **19**, 7410-7424.
13 Jieyun Wu, Hongyan Xiao, Ling Qiu, Zhen Zhen, Xinhou Liu and Shuhui Bo, RSC Adv., (2014) **4**, 49737-49744.
14 JieyunWu, Chengcheng Peng, Hongyan Xiao, Shuhui Bo, Ling Qiu, Zhen Zhen and Xinhou Liu, Dyes and Pigments, (2014) **104**, 15-23.
15 Seong-Ku Kim, H. Zhang, D. H. Chang, C. Zhang, C. Wang, W. H. Steier and H. R. Fetterman, IEEE Photon. Technol. Lett., 2003, **15**(2), 218–220.
16 Okihiro Sugihara, Shuhei Yasuda, Bin Cai, Kyoji Komatsu and Toshikuni Kaino, Optics Lett., 2008, **33**(3), 294-296.
17 Louay Eldada, Chengzeng Xu, Kelly M. T. Stengel, Lawrence W. Shacklette and James T. Yardley, J. Lightwave Technol., 1996, **14**(7), 1704–1713.
18 S.-K. Kim, K. Geary, D.H. Chang, H.R. Fetterman, H. Zhang, C. Zhang, C. Wang and W.H. Steier, Electron. Lett. **39**(9), 2003, 721-722.
19 Seong-Ku Kim, W. Yuan, K. Geary, Yu-Chueh Hung, H. R. Fetterman and Dong-Gun Lee, Appl. Phys. Lett., 2005, **87**, 011107.
20 Rogner, A. and Pannhoff, H, Optical Fiber Communication (OFC'94), San Jose, CA, USA, Tech. Digs., 1994, **4**, 279-280.
21 Youxuan Zheng, Yonghui Zhou, Gianluca Accorsi and Nicola Armaroli, J. Rare Earths, 2008, **26**, 173-177.
22 Dongfeng Fan, Xu Fei, Jing Tian, Longquan Xu, Xiuying Wang, Shuqi Fan and Yi Wang, Polym. Chem., 2015, **6**, 5430–5436.
23 Changming Chen, Xiaoqiang Sun, Fei Wang, Feng Zhang, Hui Wang, Zuosen Shi, Zhanchen Cui and Daming Zhang, IEEE J. Quantum Electron, 2012, **48**(1), 61-66.
24 S. H. Bo, J. Hu, Z. Chen, Q. Wang, G. M. Xu, X. H. Liu and Z. Zhen, Appl. Phys. B, 2009, **97**(3), 665–669.
25 Ka-Long Lei, Cheuk-Fai Chow, Kwok-Chu Tsang, Elva N. Y. Lei, V. A. L. Roy, Michael H. W. Lam, C. S. Lee, E. Y. B. Pun and Jensen Li, J. Mater. Chem., 2010, **20**, 7526–7529.
26 Yan Wang, Xingyuan Guo, Shusen Liu, Kezhi Zheng, Guanshi Qin and Weiping Qin, Journal of Fluorine Chemistry, 2015, 175, 125-128.
27 Jong-Kyun Hong and Sang-Sun Lee, IEEE J. Lightw. Technol., 2007, **25**(5), 1264–1268.
28 Young-Ouk Noh, Chul-Hee Lee, Jong-Min Kim, Wol-Yon Hwang, Yong-Hyub Won, Hyung-Jong Lee, Seon-Gyu Han and Min-Cheol Oh, Opt. Commun.,2004, **242**, 533–540.
29 Xiaoqing J, Xia L, Haifeng Z, Jianyi Y, Minghua W, Yuying W and Shigeta I, IEEE Photon. Technol. Lett., 2005, **17**, 2361–2363.
30 Jin T K, Choon-Gi C and Hee-Kyung S ETRI J.**,** 2005**, 27**, 122–125.
31 Alejandro Maese-Novo, Ziyang Zhang, Gelani Irmscher, Andrzej Polatynski, Tim Mueller, David de Felipe, Moritz Kleinert, Walter Brinker, Crispin Zawadzki and Norbert Keil, Appl. Opt., 2015, **54**(3), 569-575.

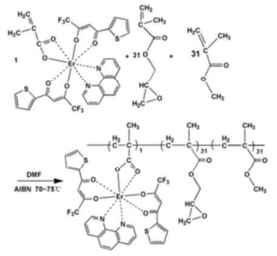

Poly(GMA-co-Er(TTA)$_2$ (Phen)(MA))

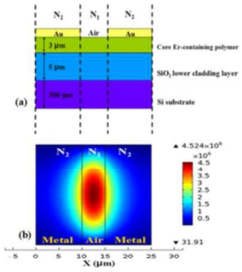

Metal-cladding directly defined active waveguide technique

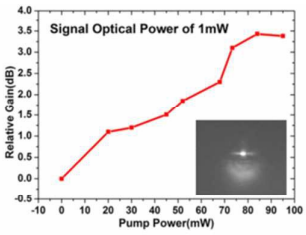

Metal-cladding directly defined polymer amplifier

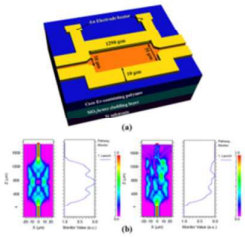

Metal-cladding self-electrode polymer TO waveguide switch

The complex Er(TTA)$_2$(Phen)(MA) is polymerized with glycidyl methacrylate (GMA) by free-radical polymerization of dilute monomer solutions. The copolymers Poly(GMA-co-Er(TTA)$_2$(Phen)(MA)) could form a highly epoxy cross-linked matrix structure, Which exhibits good chemical resistance and excellent processability. By introducing an organic ligand (methacrylic acid) with excellent polymerization activity, it can provide carboxyl groups as coordinating groups for Er^{3+}. methacrylic acid plays a dual role as an organic ligand and a compatibilizer and Er chelates can use olefinic double bonds to copolymerize with other monomers for reducing phase separation effectively between Er complexs and polymers. Based on optical characteristics and thermal stabilities of the active polymer, novel metal-cladding directly defined active waveguide technique is proposed. Optical waveguide amplifiers and thermo-optic (TO) waveguide switches based on the erbium-containing polymer are designed and fabricated using this technique. The technique is advantageous to realize a simple fabrication process for the large-scale photonic multi-functional integrated circuits (PICs) and optimize cross-connectors for OXC and OADM systems.